IEEE Access
Multidisciplinary | Rapid Review | Open Access Journal

SPECIAL SECTION ON COMMUNICATIONS IN HARSH ENVIRONMENTS

Received May 28, 2020, accepted June 15, 2020, date of publication June 25, 2020, date of current version July 7, 2020.

Digital Object Identifier 10.1109/ACCESS.2020.3004875

Thermal Stability Analysis of Filters in Substrate Integrated Technologies Under Atmospheric Pressure and Vacuum Conditions

VICENTE NOVA[1], CARMEN BACHILLER MARTIN[1], (Member, IEEE), JUAN ANGEL MARTÍNEZ[2], (Member, IEEE), HÉCTOR ESTEBAN GONZÁLEZ[1], (Senior Member, IEEE), JOSÉ MANUEL MERELLO[1], ÁNGEL BELENGUER MARTÍNEZ[2], (Senior Member, IEEE), OSCAR MONERRIS[3], AND VICENTE E. BORIA[1], (Fellow, IEEE)

[1]Instituto de Telecomunicaciones y Aplicaciones Multimedia, Universitat Politècnica de València, 46021 Valencia, Spain
[2]Instituto de Tecnología, Construcción y Telecomunicaciones, Universidad de Castilla-La Mancha, 16071 Cuenca, Spain
[3]European High Power Radiofrequency Space Laboratory, Val Space Consortium, 46022 Valencia, Spain

Corresponding author: Vicente Nova (vinogi@iteam.upv.es)

This work was supported in part by the Generalitat Valenciana Research Project PROMETEO/2019/120, in part by the Ministerio de Economía y Competitividad, Spain, through the Research and Development Project under Grant TEC2016-75934-C4-1-R, and in part by the Agencia Estatal de Investigación, Spain, through the Fellowship for Training PhDs under Grant BES-2017-079728.

ABSTRACT Substrate Integrated (SI) technologies, either completely or partially filled with dielectric, as well as completely empty (i.e. without any dielectric material), have been object of intense research in the last years. Their performance in terms of losses, cost and size are mid-way between those of classical planar lines and rectangular waveguides. Many communication devices have already been successfully designed, manufactured and measured in all these SI technologies. But these measurements are mostly done at room temperature under atmospheric pressure conditions. However, the good results (in terms of low loss, profile and cost) of these novel technologies, especially the completely empty versions, close to the performance of the rectangular waveguide, make them a very good alternative for being used in small satellite payloads. Up to now, few attention has been given to the thermal analysis of these SI technologies, still missing a complete comparative study of these effects under both, atmospheric pressure and vacuum conditions. In this work the same filter is implemented on four different SI technologies (including completely and partially filled with dielectric, as well as empty -no dielectric- versions). The four filters are designed, manufactured, and measured at different temperatures according to the thermal testing standards for space applications. The thermal study is performed under atmospheric pressure conditions and, for the first time, under high vacuum conditions. Finally, a comparison with all previous available thermal studies (all of them performed at atmospheric pressure levels) is included.

INDEX TERMS Cavities, empty substrate-integrated coaxial line (ESICL), empty substrate-integrated waveguide (ESIW), filters, microwave integrated circuits, payloads, rectangular waveguide, satellites, substrate integrated waveguide (SIW), space communications, substrate integrated circuits (SIC), thermal stability coefficient of thermal expansion (CTE).

I. INTRODUCTION

A rectangular waveguide integrated in a planar substrate, called Substrate Integrated Waveguide (SIW), was proposed in [1] as a compromise between classical planar transmission lines (such as microstrip) and other technologies with better performance, such as waveguides and coaxial lines. The main aim was to obtain high frequency circuits with higher performance than classical planar lines, but with similar features in terms of low cost, low weight and small volume. The SIW consists of a Printed Circuit Board (PCB) with two rows of metallized vias (see Fig. 1a). Thus, the field is confined by the top and bottom metal layers of the PCB and by the lateral walls formed by the rows of vias. This reduces the radiation loss compared to a microstrip line, thus increasing the quality factor of resonant cavities implemented in this

The associate editor coordinating the review of this manuscript and approving it for publication was Qiong Wu.

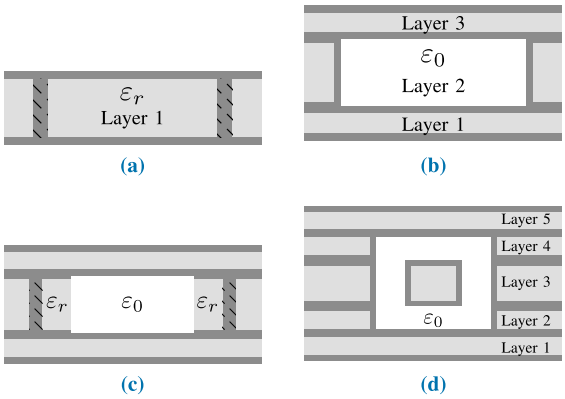

FIGURE 1. Cross-section of SI technologies considered in this work: (a) SIW, (b) ESIW, (c) AFSIW, and (d) ESICL. Light gray is the dielectric substrate, white is the empty gap, dark gray is copper, and patterns of lines are metallized vias.

SIW technology. However, the field propagates through the lossy dielectric body of the PCB, and thus, the performance in terms of losses and quality factor, even being better than in classical planar lines, is still far from the performance of high quality transmission lines such as the classical rectangular waveguide.

Much research has been devoted to design and implementation of SIW devices. In [2], a thorough review of the state of the art of SIW circuits such as filters, couplers, transitions, oscillators, mixers, amplifiers and antennas is performed. A more specific review of SIW filters can be found in [3]. Thus, SIW is a mature technology that has been successfully used for implementing a wide variety of communication devices.

In order to take a step further, some proposals of new SI transmission lines, where the dielectric body is either totally or partially removed, have recently appeared. The first of these empty SI lines, called Empty Substrate Integrated Waveguide (ESIW), was presented in [4]. The ESIW is manufactured by emptying the PCB, metallizing the walls with electrodeposition, and finally pasting a top and a bottom metallic cover (see Fig. 1b). Since the fields propagate through air, the total insertion loss is reduced, and therefore the quality factor of ESIW resonators is increased. However, the size is larger when compared to SIW, since the wavelength in air is greater than inside the dielectric of the PCB. The performance of ESIW devices in terms of losses and quality factor, is much better than those implemented in SIW technology, approaching the performance of rectangular waveguide devices, while the low cost and low profile of ESIW is similar to that of SIW. Many communication devices have also been successfully implemented in ESIW, such as transitions [5]–[8], filters of different order and frequency bands [4], [9], filters with increased height and quality factor [10], compact filters [11], [12], 90° hybrid directional couplers [13], Moreno cross-guide directional couplers [14], and antennas [15], [16].

Other similar solutions to ESIW technology have also been proposed. In [17], [18] the so-called Air-Filled Substrate Integrated Waveguide (AFSIW) was presented. As in the ESIW, the AFSIW is manufactured by emptying the PCB substrate. But in the AFSIW the lateral walls are not solid, they are built by placing rows of metallized vias in the same way as it is done for the SIW. So, the AFSIW is partially filled with dielectric, as shown in Fig. 1c. The presence of some dielectric slightly increases the losses, and the rows of vias are more complex to analyze than the solid walls, although equivalent rectangular waveguides can be used for modelling purposes. Many communication devices have also been successfully implemented with AFSIW technology [9].

Mid-way between the SIW and the empty solutions (ESIW or AFSIW) are the partially filled ESIW [19], the slab AFSIW [20], or the alternating SIW with alternating air and dielectric line sections (ADLS) [21]. These are ESIW or AFSIW versions where the waveguide is partially filled with dielectric, thus achieving performances mid-way between SIW and ESIW/AFSIW, worsening the losses and quality factor when compared to ESIW/AFSIW, but reducing the physical size.

Finally, a collection of empty SI transmission lines with two conductors has also been object of intense research. The advantage of using two conductors, instead of one as in SIW/ESIW/AFSIW, is that the fundamental mode is a TEM mode, which has wider mono-mode bandwidth and lower dispersion than the TE_{10} fundamental mode of SIW/ESIW/AFSIW. The most simple geometry of an empty substrate integrated transmission line with two conductors is that of the so-called Empty Substrate Integrated Coaxial Line (ESICL) [22]–[24], whose cross section is depicted in Fig. 1d. An ESICL version partially filled with dielectric has also been proposed [25], as well as ESICL manufactured with 3D printing [26]. Several communication devices have been also successfully implemented with ESICL, such as filters [23], [27], compact filters [28], [29], power dividers, or 90° hybrid directional couplers [30].

These technologies, especially the empty ones such as ESIW or ESICL, have performances close to those of the high quality rectangular waveguides, and they are low cost and low profile. Therefore, they are perfect candidates for being used in the payload of low-orbit small-satellite constellations that are required for the Internet the Things (IoT) [31], [32]. However, although many communication devices have already been successfully implemented with SI technologies (either filled, empty, or partially filled with dielectric), few tests have been made in order to validate these technologies for space applications, where the devices have to stand extreme temperature variations and high-vacuum conditions.

In [33], the thermal behaviour of a SIW filter with 6 resonators within the temperature range from −30°C to +65°C, under atmospheric pressure, is presented. It concludes that the thermal stability is similar to that of the same filter implemented with the classical planar microstrip technology.

The thermal stability of SIW filters is also discussed in [34], and the behaviour of a SIW filter and the equivalent filter in microstrip are analyzed from −40°C to +85°C, under atmospheric pressure. The insertion loss of the SIW filter is more stable than for the microstrip one, due to the greater isolation of the SIW structure, which makes this technology less sensitive to moisture.

As temperature changes, the permittivity of the PCB substrate changes, but there is also an expansion or contraction of the substrate that changes the size of the resonators in a filter. A proper selection of the substrate is done in [35], so that the thermal expansion and the thermal drift of the permittivity are compensated, thus producing SIW filters with very stable thermal behaviour. The same procedure is done in [36] for AFSIW filters. This is possible because AFSIW is partially filled with dielectric, and, in order to obtain a thermally stable filter, a significant portion of the filter has to be filled with dielectric, thus increasing the loss compared with the same filter in the alternative ESIW technology. In both [35] and [36], the measurements are made from −40°C to +80°C, under atmospheric pressure conditions.

However, for space applications, the thermal behaviour of communication devices has to be tested not only under atmospheric pressure, but also in vacuum, as specified in the standards of the European Cooperation for Space Standardization (ECSS) space tests sheets [37].

In this work, we analyze the thermal behaviour of the same directly coupled cavities filter implemented in several filled, partially filled, and completely empty substrate integrated technologies (i.e. SIW, ADLS, ESIW and ESICL) under atmospheric pressure and high-vacuum conditions. For this purpose, we have considered temperature profiles for real satellite payloads.

II. SUBSTRATE INTEGRATED FILTERS IN SIW, ADLS, ESIW AND ESICL

Four different filters, all of them with the same specifications (five poles, Chebyshev response with 0.1 dB of ripple and return loss level of 25 dB in the pass-band, centered at 13 GHz with 400 MHz of bandwidth), have been designed and manufactured in four different SI technologies: SIW, ESIW, ADLS, and ESICL. Fig. 2 shows the layout of the central layer of these filters. In order to be integrated with planar circuits, transitions from microstrip to each one of these SI transmission lines have also been designed, as shown in Fig. 2.

All filters have been manufactured with RO4003C substrate, with a relative permittivity of 3.38 and a loss tangent of 0.0027, both at 10 GHz. Thus, the same thermal expansion coefficient of the substrate can be applied to all of them. Nevertheless, since they have different topologies, it would be interesting to investigate the thermal behavior of each one. In the case of ESIW and ESICL filters, the permittivity of the substrate is only relevant for the design of transitions since they are empty structures. The dimensions of the filters are displayed in Tables 1 to 5.

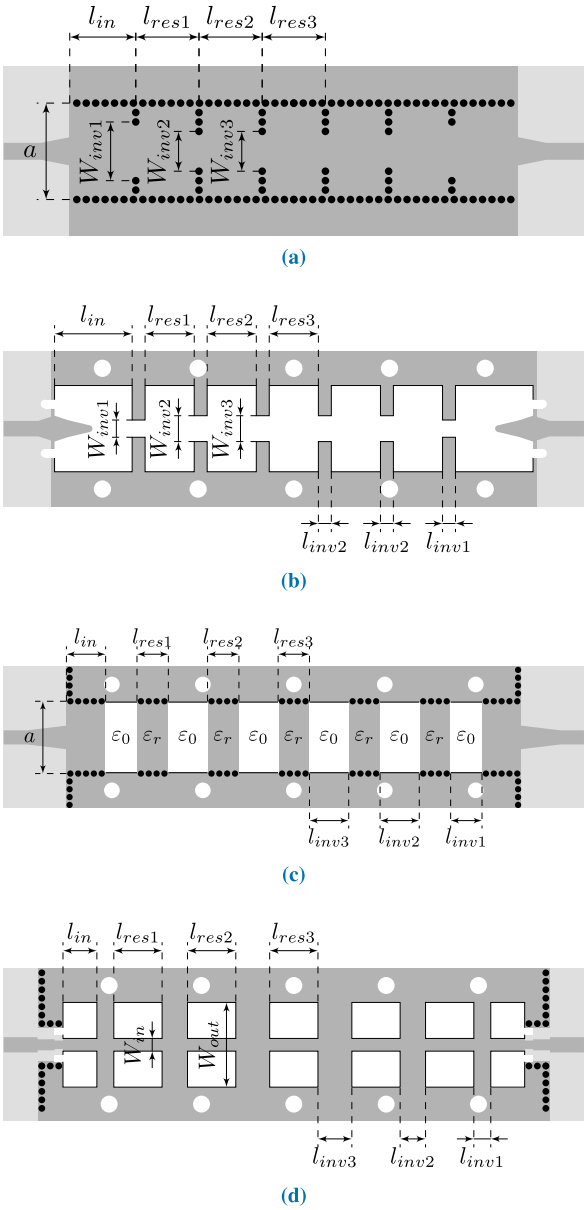

FIGURE 2. Layout of the central layer of the four filters: (a) SIW, (b) ESIW, (c) ADLS, and (d) ESICL. Light gray is the dielectric substrate, white is the empty gap, dark gray is copper, black circles are metallized vias, and black lines are metallized walls.

TABLE 1. Overall size of the filters.

Filter	Height (mm)	Width (mm)	Length with transitions (mm)
SIW	1	25	90
ESIW	3	40	140
ADLS	3	25	113
ESICL	4	20	116

III. MEASUREMENTS SET UP

Temperature tests are required to validate the good performance of microwave devices for space applications. These tests evaluate the variation of the frequency response of space payload devices within a wide temperature range. In this case,

TABLE 2. Dimensions (in mm) of the SIW filter.

W_{inv1}	4.978	l_{res1}	8.076
W_{inv2}	3.363	l_{res2}	8.898
W_{inv3}	3.061	l_{res3}	8.933.
l_{in}	10	a	8.931
p	1	d	0.7

TABLE 3. Dimensions (in mm) of the ESIW filter.

W_{inv1}	8.969	l_{res1}	13.584
W_{inv2}	6.053	l_{res2}	15.286
W_{inv3}	5.488	l_{res3}	15.476
l_{inv1}	2	l_{in}	15
l_{inv2}	2	l_{inv3}	2

TABLE 4. Dimensions (in mm) of the ADLS filter.

l_{res1}	3.181	l_{inv1}	4.877
l_{res2}	3.104	l_{inv2}	10.654
l_{res3}	3.099	l_{inv3}	12.059
a	8.3851	l_{in}	10
d	0.7	p	1

TABLE 5. Dimensions (in mm) of the ESICL filter.

l_{res1}	9.189	l_{inv1}	1.316
l_{res2}	9.317	l_{inv2}	5.203
l_{res3}	9.319	l_{inv3}	6.025
W_{in}	1.808	l_{in}	10
W_{out}	6		

the four manufactured filters were subject to two tests: under atmospheric pressure and high vacuum conditions. In each test different measurement setups, and therefore, different temperature profiles were applied.

A. SET-UP FOR TESTS UNDER ATMOSPHERIC PRESSURE CONDITIONS

These tests have been performed following the technical specifications for testing the different systems and devices used for space engineering [37]. In particular, those required for the standardization of payload equipment, generally including waveguides and waveguide based devices, as it is the case of the considered filters.

The range of temperatures is from −40 to +70°C, including measurements at −35, −25, +60°C and room temperature (+25°C), see Fig. 3. This temperature profile is compliant with the requirements of ECSS for thermal tests under atmospheric pressure conditions.

The measurement set up consists of a temperature chamber (Vötsch VT70010) and a vector network analyzer (VNA). Inside the thermal chamber there are two temperature sensors, one on a chamber wall and the other on the device under test (DUT).

The measurement consisted on introducing the devices, one by one, inside the thermal chamber while they are connected to the VNA (this set-up is similar to the one of the vacuum tests, see Fig. 4). The thermal chamber adapted the

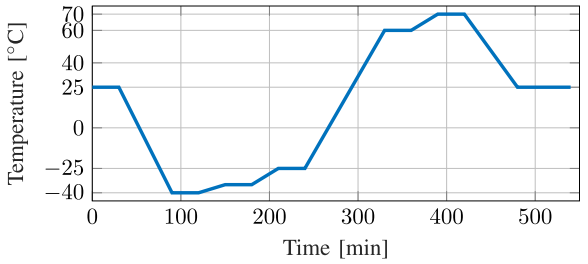

FIGURE 3. Temperature profile for tests under atmospheric pressure conditions.

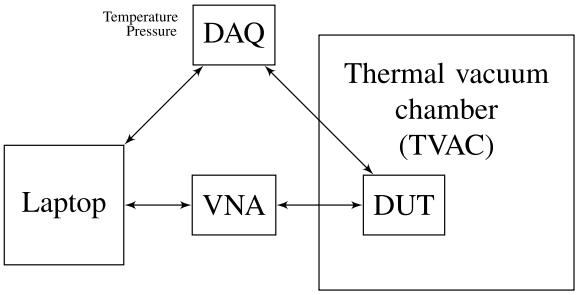

FIGURE 4. Measurement set-up diagram for vacuum temperature tests.

temperature of the device to the target temperature of the profile. Every time the temperature has reached one of the the targets in the profile, the electric response of the device is stored after a dwell time.

A TRL calibration kit was developed, but the VNA was not calibrated before measuring the filters, since that would assume that the responses of the TRL calkit standards (Thru, Reflect and Line) do not change with temperature. In fact, the electric responses of these three calkit elements were measured at each one of the target temperatures. Thereafter, these measurements are used to calibrate the responses of the four different filters by using a Matlab program, that allows to obtain the corrected measurement at each one of the temperatures following the procedure described in [38].

In a first attempt, screwed end-launch connectors were used, nevertheless, the connectors did not work near −40°C. The different expansion coefficients of the connectors and the substrate causes movements between its different parts and, as a consequence, the active conductor of the connector no longer touched the input microstrip line. Therefore, welded SMA connectors with a working temperatur range from −65°C to +165°C were finally used.

B. SET-UP FOR VACUUM TESTS

Thermal vacuum testing shall be performed for space devices whose normal operation occurs in space vacuum environment at any time of their lifetime [37]. The pressure of this test shall be maintained under 10^{-5} hPa. For this reason, an ad-hoc vacuum system consisting of a turbomolecular pump and a primary vacuum pump was used. The measurement system can be seen in Fig. 4, the lower limit of this setup was −80°C

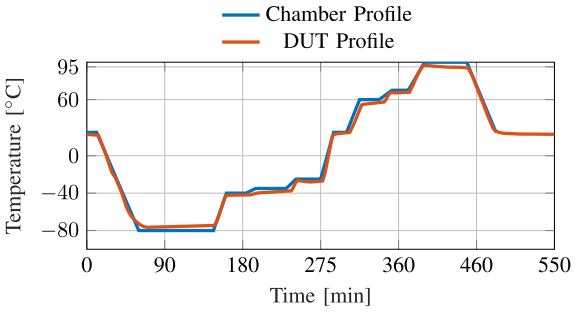

FIGURE 5. Measured temperature profiles used in all the vacuum measurements for DUTs and TRL standards.

and the upper temperature was limited to +100°C, since the soldering of the connectors can cause outgassing at higher temperature and the vacuum chamber can be contaminated.

Measurements at the same intermediate temperatures used for the atmosphere tests were set up in the profile, but in this case more target temperatures are considered. The final set of temperatures was −80, −40, −35, −25, +25, +60, +70 and +100°C, see Fig. 5. The greatest temperature slope in the profile is 5°C/min, so the compliance with the ECSS normative [37] is achieved by far.

It is important to notice that, under high-vacuum conditions, the heat transmission only occurs via conduction and radiation. Thus, measuring a temperature in the thermal vacuum chamber (TVAC) does not ensure the same temperature in the devices. For this reason, three thermal sensors have been attached in different parts of the DUT. One sensor is placed on the TVAC base plate, the other one on the body of the DUT and a third one close to the input DUT connector. Moreover, in the case of measurements in absence of atmosphere, the transmission of heat from the thermal base of the TVAC to the device must be guaranteed by means of a heat transmission material. In this case, two types of test jigs have been used in order to promote the heat transmission:

- *Test jig*. Aluminium jigs were used to fix the devices to the base of the thermal chamber. These bases have slots for fixing them to the thermal chamber and holes that allow to fix the DUTs to the base itself using plates, see Figs. 6a and 6b. This kind of supports can be used for large devices, as filters, but not for the small standards of the TRL calibration kit.
- *Copper thermal "bridge"*. This type of support is formed by a copper sheet to which the elements of the TRL calibration kit are welded. This support can be screwed to the TVAC base allowing heat to flow to the device, see Fig. 6c.

A test was performed with a ''dummy'' device to check if the heat propagates correctly. As shown in Fig. 5, although the programmed temperature profile ranged from −80 to +100°C, the sensor placed on the DUT with the integration jig measured a minimum temperature of −75°C, and a maximum of +95°C. The sensors on the DUT and the connectors

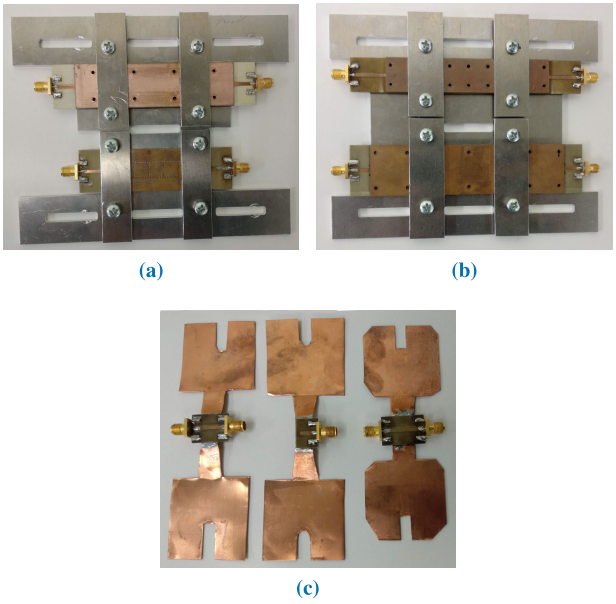

FIGURE 6. Test jigs: (a) ADLS and SIW filters on aluminium jigs, (b) ESIW and ESICL filters on aluminium jigs, and (c) TRL CalKit elements on copper thermal bridge.

proved that the thermal ''bridges'' work well for large size devices such as the TRL line standard or the dummy DUT, but they do not work very well with smaller devices such as the TRL open or thru standards for very low temperatures. The open standard only reached −65°C. Therefore, the range of temperatures in which it is possible to make a correctly calibrated measurement is limited to a range from −65 to +95°C. Nevertheless, this range is compliant with the ECSS vacuum tests requirements.

IV. RESULTS

A. SIMULATION

An estimation of the frequency drift in the scattering parameters of the filters, as a consequence of the temperature variations, was performed prior to measurements. In this project, RO4003C material from the Rogers corporation was employed, $\varepsilon_r = 3.38$, and lost tangent of 0.0027 at 10 GHz, with copper cladding of 35 μm whose conductivitty is 5.8×10^7 S/m. Concerning the behaviour with the temperature, the material has a thermal coefficient of $\varepsilon_r = +40$ ppm/°C, measured in a range from −50 to +150°C, and coefficients of thermal expansion (CTE) of 11, 14 and 46 ppm/°C for the X, Y and Z dimensions, respectively, in the range from −55 to +288°C. The manufacturer does not provide thermal coefficient for the loss tangent. However, as it can be seen in the measured results, the temperature also impacts on the loss related to the dielectric material.

In order to estimate the frequency response variation with the temperature, each filter was simulated using the commercial software CST Studio Suite (v. 2019, from Dassault Systèmes) at five different temperatures (−60, −40, +25, +70, and +95 °C) which correspond to room temperature and to the extreme values of both, the atmospheric and the

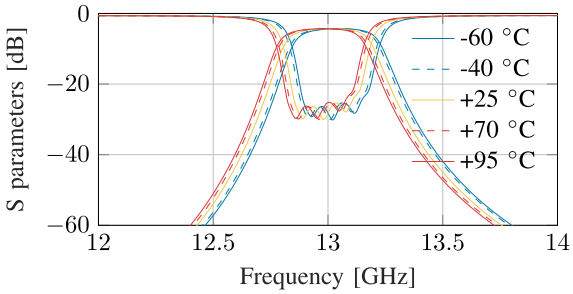

FIGURE 7. Simulated result for temperature variation in SIW filter.

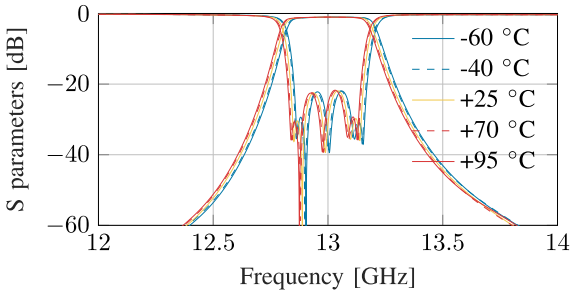

FIGURE 8. Simulated result for temperature variation in ESIW filter.

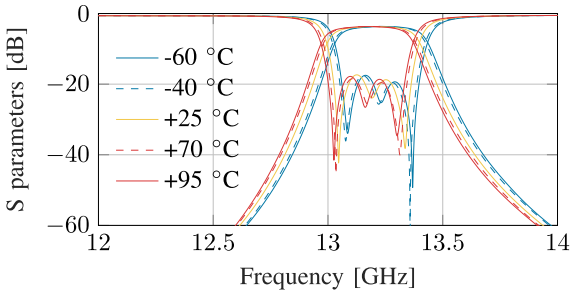

FIGURE 9. Simulated result for temperature variation in ADLS filter.

vacuum tests. For each temperature value, the effects of both, the thermal coefficient of ε_r and the thermal expansion coefficients in X, Y and Z, were taken into account in the simulations of the filters. It is important to notice that in the case of the ESIW and ESICL filters, since they are completely empty of dielectric, the thermal coefficient of ε_r only affects to the microstrip transitions. The results of such simulations are displayed in Figs. 7, 8, 9 and 10.

As it can be observed in Fig. 7, the simulation for the SIW filter estimates a frequency drift of +27 MHz at −40 °C and of −19 MHz at +70 °C, the extreme temperatures of the atmosphere test. Moreover, a frequency drift of +39 MHz is expected at −60 °C and of −30 MHz at +95 °C, the extreme temperatures of the vacuum test.

Regarding the ESIW filter, see Fig. 8, the estimation is a frequency drift of +11 MHz at −40 °C and −8 MHz at +70 °C, and +15 MHz at −60 °C and −12 MHz at +95 °C.

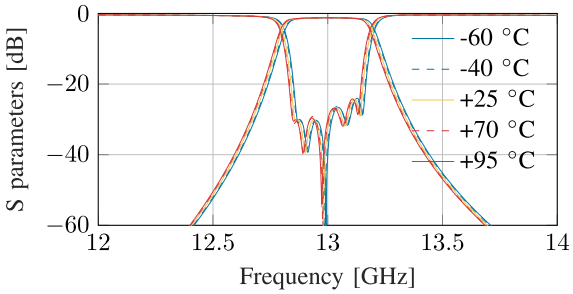

FIGURE 10. Simulated result for temperature variation in ESICL filter.

Although all filters were designed to have the same frequency response, the manufactured ADLS filter presented a frequency shift (as can be seen in measurements of Fig. 12). This shift (from 13 GHz to 13.2 GHz) is due to the assembling process, particularly to a reduction of 20 μm in the expected thickness of the welding layer that can not be manually controlled. Accordingly, the simulated response of the ADLS topology takes into account this reduction of the welding layer, and the simulated central frequency at room temperature is 13.2 GHz (Fig. 9). The simulation with temperature variation gives a frequency drift of +25 MHz at −40 °C and −17 MHz at +70 °C, and a frequency drift of +34 MHz and −12 MHz at −26 °C and +95 °C, respectively.

Finally, the simulated frequency drift of the ESICL filter is +8 MHz at −40 °C, −6 MHz at +70 °C, +11 MHz at −60 °C, and −9 MHz at +95 °C, see Fig. 10.

B. MEASUREMENTS IN ATMOSPHERIC PRESSURE CONDITIONS

Figures 11, 12, 13 and 14 depict the transmission and reflection coefficients of the four filters after applying the external TRL temperature calibration procedure at each temperature, under atmospheric pressure.

As expected, lowering the temperature increases the central frequency of the filter, whilst increasing the temperature lowers it. This effect is appreciated in all the filters, since it responds mainly to the size variation that the filters experiment with the temperature gradient. SIW filter presents a drift of +23 MHz at −40°C and −14 MHz at +70°C. ADLS filter presents a drift of +19 MHz at −40°C and −12 MHz at +70°C. ESIW filter, a drift of +11 MHz at −40°C and −8 MHz at +70°C, and ESICL filter, a drift of +13 MHz at −40°C and −7 MHz at +70°C, the ones with less variation, since these two filters are empty and a temperature deviation only affects the dimensions of the filter. Moreover, there is an interesting effect that is observed only in ADLS and SIW filters, which is the increment of the losses when the temperature increases. This effect is mainly due to the presence of a loss thermal coefficient in the dielectric material. As it can be observed, in the measurements of the filters on empty transmission lines (ESIW and ESICL), this effect is negligible.

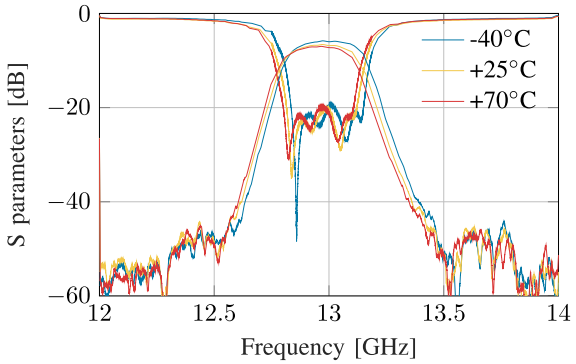

FIGURE 11. SIW filter temperature results under atmospheric pressure.

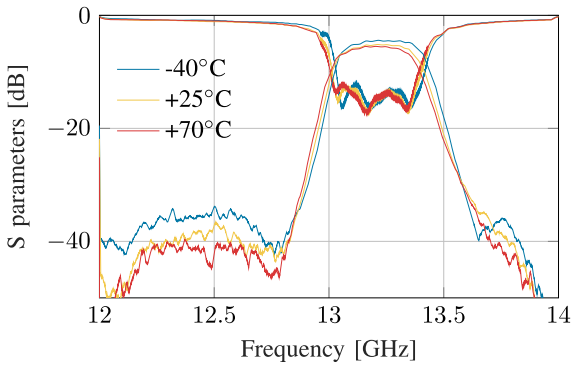

FIGURE 12. ADLS filter temperature results under atmospheric pressure.

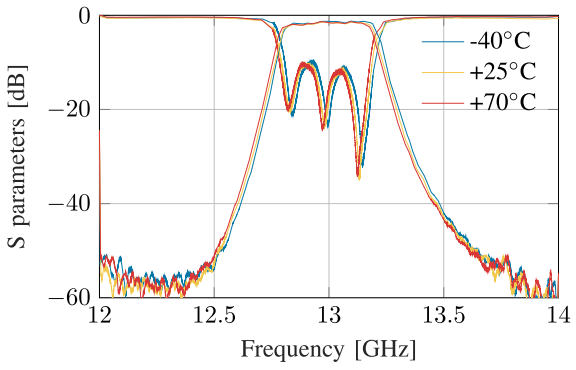

FIGURE 13. ESIW filter temperature results under atmospheric pressure.

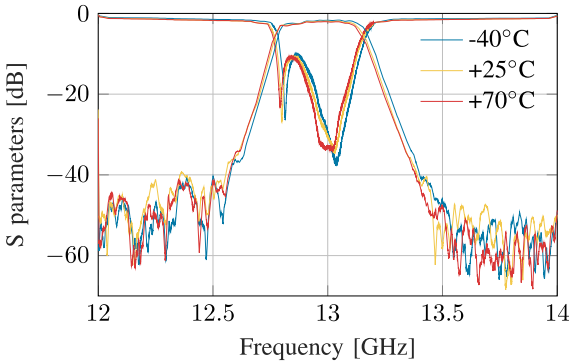

FIGURE 14. ESICL filter temperature results under atmospheric pressure.

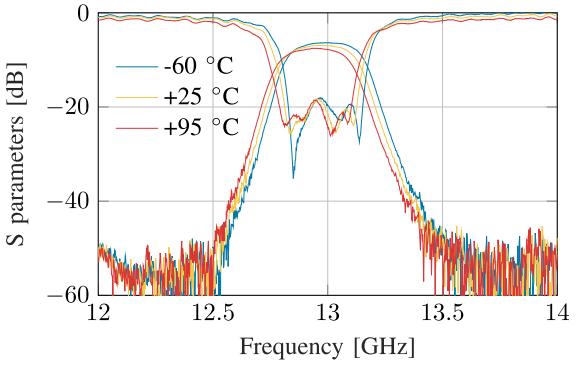

FIGURE 15. SIW filter temperature results under vacuum conditions.

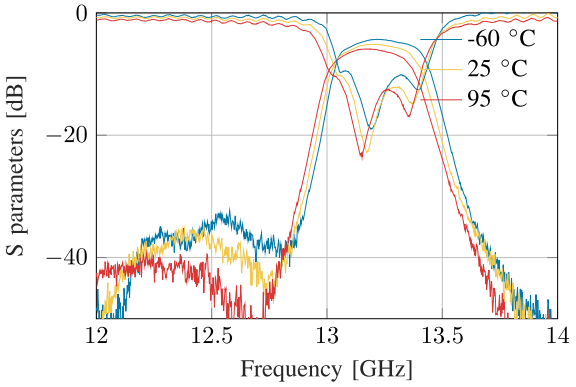

FIGURE 16. ADLS filter temperature results under vacuum conditions.

C. MEASUREMENTS IN VACUUM

Figures 15, 16, 17 and 18 depict the shift of the transmission and reflection coefficients of the filters with the temperature in vacuum. SIW filter presents a drift of 22 MHz at −60°C and −24 MHz at +95°C. ADLS filter presents a drift of 20 MHz at −60°C and −23 MHz at +95°C. ESIW filter, a drift of 15 MHz at −60°C and −21 MHz at +95°C, and ESICL filter, a drift of −1 MHz at −60°C and −15 MHz at +95°C. The results are very similar to those of the tests under atmospheric pressure conditions, as well as to the corresponding simulations. As expected, lowering the temperature increases the central frequency of the filter, whilst increasing the temperature lowers it.

V. INSERTION LOSS ANALYSIS

Previous sections have examined the frequency and bandwidth temperature drift of the filters under high vacuum and atmospheric pressure. However, as can be seen in previous measurements, heating also has a strong impact on the insertion loss (IL) of non-empty filters: SIW and ADLS.

On the one hand, the IL of these non-empty filters in the vacuum test is slightly higher than in the atmospheric

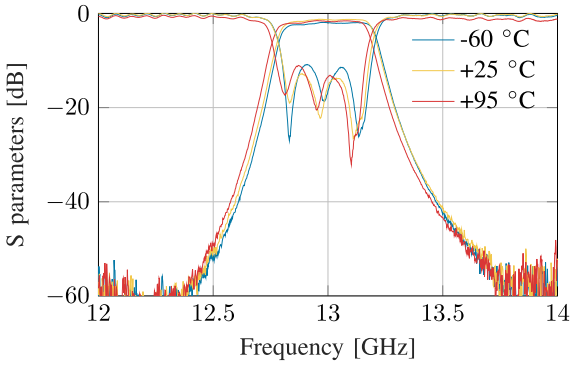

FIGURE 17. ESIW filter temperature results under vacuum conditions.

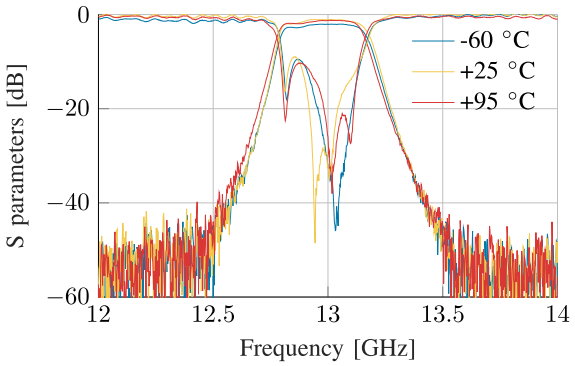

FIGURE 18. ESICL filter temperature results under vacuum conditions.

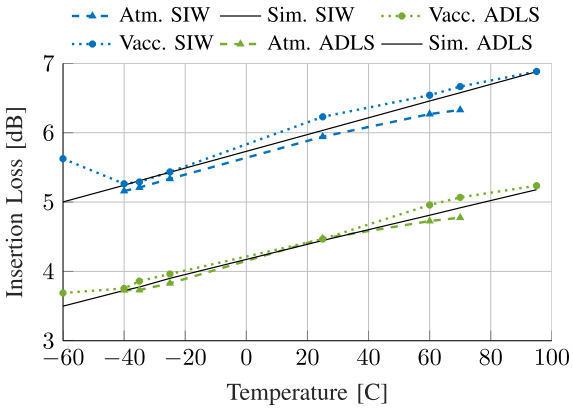

FIGURE 19. Average insertion loss of SIW and ADLS filters at different temperatures under vacuum and atmospheric conditions.

one, see Fig. 19. Moreover, measured losses in these two tests are also higher than the simulated ones. However, this effect is not observed in empty filters (ESIW and ESICL), where measured losses in both tests are in good agreement with the simulations. Thus, the change in the IL must be related to a change in dielectric properties. Since filters were heated to temperatures up to 230 °C during the manufacturing process before being tested (firstly under atmospheric presure and afterward in vacuum condition), these high temperature gradients should have permanently increased the loss tangent of RO4003C. Thereby, a new loss tangent value of RO4003C substrate was extracted from measurements, by fitting measured and simulated IL at 25 °C, obtaining a final value of approximately 0.0045.

On the other hand, as can be seen in Fig. 19, there is an IL drift with temperature variation. In the case of filled filters, the maximum IL drift are: 0.0125 dB/°C, and 0.0108 dB/°C for SIW and ADLS filter, respectively. Whereas, in the case of ESIW and ESICL they are 0.0023 dB/°C and 0.0034 dB/°C, respectively. As can be expected, empty filters topology has lower variation in IL, since it is only due to a variation of the copper conductivity, whereas filled filters also have a drift in dielectric loss term.

In order to extract an approximation of the thermal coefficient of RO4003C loss tangent, an iterative optimization process was used. In this optimization process, a 3D electromagnetic model was simulated in CST in order to fit the simulated and measured loss variation between −40 °C and +95 °C. The electromagnetic simulation includes the following parameters: the previous considered thermal expansion and permittivity variation coefficients of RO4003C substrate, the previously extracted loss tangent value for the heated substrate ($\tan(\delta) = 0.0045$), and the thermal resistivity coefficient of standard copper (3930 ppm/°C). The optimization process started with the average thermal coefficient of the measured IL. The value of the thermal coefficient for the loss tangent was optimized using the Trust Region Framework, obtaining a final value of 2200 ppm/°C.

VI. COMPARISON AND DISCUSSION

Table 6 provides a comparative study of the results for the SIW, ADLS, ESIW and ESICL filter prototypes presented in this work, together with the results of a similar filter manufactured in WR42 rectangular waveguide [38], an ESIW filter presented in [36], and self-compensated SIW and AFSIW filters presented, respectively, in [35] and [36].

Results presented in Table 6 show that, as expected, the empty substrate integrated structures (ESIW, AFSIW and ESICL) have less frequency and bandwidth deviation with temperature than the ones totally or partially filled with substrate (SIW and ADLS), affected by the thermal coefficient of the dielectric permittivity. This effect is taken into account in the SIW and AFSIW compensated filters with the proper selection of the dielectric, with a thermal coefficient that compensates the thermal expansion of the substrate. The price to pay for this compensation is an increase in the insertion losses. The rectangular waveguide (WR42) filter, although it is completely empty of dielectric, presents similar deviation with the temperature to ESIW and ESICL because the rectangular waveguide is manufactured by milling an aluminium block, while ESIW and ESICL are manufactured emptying a PCB substrate and metallizing the walls. It must be taken into account that the expansion coefficient of aluminium is 24 ppm/°C, much more than that of the

TABLE 6. Comparison of results.

Technology	f_0 GHz (25°C)	Order	IL dB (25°C)	FBW (%) (25 °C)	Temp.	Δf_0 %	ΔBW %	ΔIL %	Planar Integration	Atmosphere tests	Vacuum tests
WR 42 [38]	18.382	2	0.3903	2.47	100	-0.1286	0.1927	8.7798	No	Yes	No
Compensated SIW [35]	10.065	4	0.5	11.6	-40 80	-0.059 0.050	-4.22 -3.965	-40 40	Yes	Yes	No
Compensated AFSIW [36]	21.003	4	1.080	1.600	-40 80	-0.014 0.010	2.380 0.595	-23.14 6.48	No[2]	Yes	No
ESIW [36]	21.006	4	0.700	1.59	-40 80	0.109 -0.105	-0.898 -0.299	-12.857 5.714	No[2]	Yes	No
SIW[1]	12.966	5	6.085	2.422	-60 95 -40 70	0.1693 -0.185 0.180 -0.114	2.548 -2.548 4.048 0.2004	-8.350 9.056 -11.277 5.566	Yes	Yes	Yes
ESIW[1]	12.993	5	0.625	3.125	-60 95 -40 70	0.1154 -0.1618 0.0854 -0.0625	1.4778 0.4926 1.087 -0.2415	47.463 23.772 -14.225 -3.516	Yes	Yes	Yes
ADLS[1]	13.213	5	4.470	2.695	-60 95 -40 70	0.1505 -0.1738 0.14 -0.091	4.4944 -1.6854 2.811 -2.09	-14.218 14.08 -13.624 5.485	Yes	Yes	Yes
ESICL[1]	12.982	5	0.801	2.943	-60 95 -40 70	-0.0074 -0.1148 0.1065 -0.0549	-1.5707 -3.664 0.1646 -0.5268	66.818 12.244 -8.816 7.426	Yes	Yes	Yes

[1] The effect of transitions has been removed from measured data (It involves a reduction of 1dB in insertion loss) [4].
[2] Compensated AFSIW and ESIW from [36] have no transition to a planar line, but they are mounted on WR-51 test fixture.

RO4003 substrate. However, it should be also noticed that in the case of the WR42, the compensated AFSIW, and the ESIW filter of [36], there is no integration with planar technologies, since a waveguide is used as feeding line, instead of a planar microstrip or coplanar line, as in the case of the other filters. It should also be noted that only in the four filters presented in this work, tests have been made in vacuum conditions, not only in atmosphere pressure.

The table also shows that the relative insertion loss deviation (ΔIL %) is higher for ESIW and ESICL. Nevertheless it has to be taken into account that these values are computed comparing to the IL values at 25 °C, which are lower for ESIW and ESICL filters, as displayed in Figures 11-14 and 15-18.

After analysing the results presented in Table 6, it can be concluded that there is a full suite of possible SI technologies, some of them with very similar performances to those of the classical high quality rectangular waveguide, but with lower manufacturing cost and profile. The selection of a specific SI technology depends on the application, since there is a compromise between thermal stability, insertion loss and size. With more dielectric inside the propagation channel, physical size can be reduced and thermal stability increased (with the proper selection of the dielectric material), but at the cost of increasing the insertion loss and reducing the quality factor of the resonators.

Finally, the deviation with temperature is not too large in any of the SI technologies under study in this work. Moreover, the frequency and bandwith deviation can be compensated, as stated in [36], by using a substrate with a negative permittivity thermal coefficient. This enables the use of all these technologies in a huge number of applications, operating under atmospheric pressure and high-vacuum environments, including space communications.

VII. CONCLUSIONS

In this work, a complete thermal analysis (under atmospheric pressure and high-vacuum conditions) has been performed for the same 5-pole band-pass filter in four different SI technologies (SIW, ADLS, ESIW and ESICL). The filters have been designed, manufactured and measured at different temperatures according with the ECSS data sheet specifications for thermal testing of devices to be used in real space applications. The measurements and the simulations are in good agreement. The measured results have been compared with those of a rectangular waveguide and compensated versions of SI technologies (SIW and AFSIW). Moreover, a loss drift analysis has been done, extracting a first approximation of the thermal coefficient of RO4003C loss tangent. Even though this was not the aim of this work, this first approximation can be useful to perform a further study. With the use of a dielectric material in a substrate integrated structure, the whole size is reduced (when compared to an empty -no dielectric- implementation), at the cost of increasing losses. It has been demonstrated that ESIW and ESICL have similar thermal stability than a rectangular waveguide, due to the lower thermal expansion of the substrate compared with aluminium. The four tested SI technologies are proved to have acceptable levels of thermal stability, and they are therefore good candidates for space applications, specially in the payload of small satellites where size, cost, and weight specifications are so critical.

ACKNOWLEDGMENT

The authors gratefully acknowledge the European High Power RF Space Laboratory and the European High Power Space Materials Laboratory of Val Space Consortium for their contribution - Laboratories co-funded by the European Regional Development Fund - A way of making Europe.

REFERENCES

[1] D. Deslandes and K. Wu, "Integrated microstrip and rectangular waveguide in planar form," *IEEE Microw. Wireless Compon. Lett.*, vol. 11, no. 2, pp. 68–70, Feb. 2001.

[2] M. Bozzi, A. Georgiadis, and K. Wu, "Review of substrate-integrated waveguide circuits and antennas," *IET Microw., Antennas Propag.*, vol. 5, no. 8, pp. 909–920, Jun. 2011.

[3] X.-P. Chen and K. Wu, "Substrate integrated waveguide filters: Design techniques and structure innovations," *IEEE Microw. Mag.*, vol. 15, no. 6, pp. 121–133, Sep. 2014.

[4] A. Belenguer, H. Esteban, and V. E. Boria, "Novel empty substrate integrated waveguide for high-performance microwave integrated circuits," *IEEE Trans. Microw. Theory Techn.*, vol. 62, no. 4, pp. 832–839, Apr. 2014.

[5] H. Peng, X. Xia, J. Dong, and T. Yang, "An improved broadband transition between microstrip and empty substrate integrated waveguide," *Microw. Opt. Technol. Lett.*, vol. 58, no. 9, pp. 2227–2231, Sep. 2016. [Online]. Available: https://onlinelibrary.wiley.com/doi/abs/10.1002/mop.30015

[6] H. Esteban, A. Belenguer, J. R. Sanchez, C. Bachiller, and V. E. Boria, "Improved low reflection transition from microstrip line to empty substrate-integrated waveguide," *IEEE Microw. Wireless Compon. Lett.*, vol. 27, no. 8, pp. 685–687, Aug. 2017.

[7] Z. Liu, J. Xu, and W. Wang, "Wideband transition from microstrip Line-to- empty substrate-integrated waveguide without sharp dielectric taper," *IEEE Microw. Wireless Compon. Lett.*, vol. 29, no. 1, pp. 20–22, Jan. 2019.

[8] A. A. Khan, M. K. Mandal, and R. Shaw, "A compact and wideband SMA connector to empty substrate integrated waveguide (ESIW) transition," in *IEEE MTT-S Int. Microw. Symp. Dig.*, Dec. 2015, pp. 246–248.

[9] A. Belenguer, H. Esteban, A. L. Borja, and V. E. Boria, "Empty SIW technologies: A major step toward realizing low-cost and low-loss microwave circuits," *IEEE Microw. Mag.*, vol. 20, no. 3, pp. 24–45, Mar. 2019.

[10] J. A. Martinez, J. J. de Dios, A. Belenguer, H. Esteban, and V. E. Boria, "Integration of a very high quality factor filter in empty substrate-integrated waveguide at *Q*-band," *IEEE Microw. Wireless Compon. Lett.*, vol. 28, no. 6, pp. 503–505, Jun. 2018.

[11] J. A. Ballesteros, E. Diaz-Caballero, M. D. Fernandez, H. Esteban, A. Belenguer, and V. E. Boria, "Performance comparison of a four-pole folded filter realized with standard and empty substrate integrated waveguide technologies," in *Proc. 47th Eur. Microw. Conf. (EuMC)*, Oct. 2017, pp. 412–415.

[12] A. Belenguer, M. D. Fernandez, J. A. Ballesteros, J. J. de Dios, H. Esteban, and V. E. Boria, "Compact multilayer filter in empty substrate integrated waveguide with transmission zeros," *IEEE Trans. Microw. Theory Techn.*, vol. 66, no. 6, pp. 2993–3000, Jun. 2018.

[13] M. D. Fernandez, J. A. Ballesteros, and A. Belenguer, "Design of a hybrid directional coupler in empty substrate integrated waveguide (ESIW)," *IEEE Microw. Wireless Compon. Lett.*, vol. 25, no. 12, pp. 796–798, Dec. 2015.

[14] E. Miralles, A. Belenguer, H. Esteban, and V. E. Boria, "Cross-guide moreno directional coupler in empty substrate integrated waveguide," *Radio Sci.*, vol. 52, no. 5, pp. 597–603, May 2017. [Online]. Available: https://agupubs.onlinelibrary.wiley.com/doi/abs/10.1002/2017RS006244

[15] J. Mateo, A. M. Torres, A. Belenguer, and A. L. Borja, "Highly efficient and well-matched empty substrate integrated waveguide H-Plane horn antenna," *IEEE Antennas Wireless Propag. Lett.*, vol. 15, pp. 1510–1513, 2016.

[16] E. Miralles, A. Belenguer, J. Mateo, A. Torres, H. Esteban, A. L. Borja, and V. Boria, "Slotted ESIW antenna with high efficiency for a MIMO radar sensor," *Radio Sci.*, vol. 53, no. 5, pp. 605–610, May 2018. [Online]. Available: https://agupubs.onlinelibrary.wiley.com/doi/abs/10.1002/2017RS006461

[17] F. Parment, A. Ghiotto, T.-P. Vuong, J.-M. Duchamp, and K. Wu, "Broadband transition from dielectric-filled to air-filled substrate integrated waveguide for low loss and high power handling millimeter-wave substrate integrated circuits," in *IEEE MTT-S Int. Microw. Symp. Dig.*, Jun. 2014, pp. 1–3.

[18] F. Parment, A. Ghiotto, T.-P. Vuong, J.-M. Duchamp, and K. Wu, "Air-filled substrate integrated waveguide for low-loss and high power-handling millimeter-wave substrate integrated circuits," *IEEE Trans. Microw. Theory Techn.*, vol. 63, no. 4, pp. 1228–1238, Apr. 2015.

[19] K. A. Khanjar and T. Djerafi, "Partially dielectric-filled empty substrate integrated waveguide design for millimeter-wave applications," *Prog. Electromagn. Res. C*, vol. 87, pp. 135–146, 2018.

[20] N.-H. Nguyen, A. Ghiotto, T.-P. Vuong, A. Vilcot, F. Parment, and K. Wu, "Slab air-filled substrate integrated waveguide," in *IEEE MTT-S Int. Microw. Symp. Dig.*, Jun. 2018, pp. 312–315.

[21] J. R. Sanchez, C. Bachiller, M. Julia, V. Nova, H. Esteban, and V. E. Boria, "Microwave filter based on substrate integrated waveguide with alternating dielectric line sections," *IEEE Microw. Wireless Compon. Lett.*, vol. 28, no. 11, pp. 990–992, Nov. 2018.

[22] N. A. Murad, M. J. Lancaster, Y. Wang, and M. L. Ke, "Micromachined rectangular coaxial line to ridge waveguide transition," in *Proc. IEEE 10th Annu. Wireless Microw. Technol. Conf.*, Apr. 2009, pp. 1–5.

[23] A. Belenguer, A. L. Borja, H. Esteban, and V. E. Boria, "High-performance coplanar waveguide to empty substrate integrated coaxial line transition," *IEEE Trans. Microw. Theory Techn.*, vol. 63, no. 12, pp. 4027–4034, Dec. 2015.

[24] N. Jastram and D. S. Filipovic, "PCB-based prototyping of 3-D micromachined RF subsystems," *IEEE Trans. Antennas Propag.*, vol. 62, no. 1, pp. 420–429, Jan. 2014.

[25] M. A. Al-Tarifi and D. S. Filipovic, "All-PCB transmission line with low loss and dispersion up to Ka band," in *Proc. IEEE Antennas Propag. Soc. Int. Symp. (APSURSI)*, Jul. 2014, pp. 826–827.

[26] G. Venanzoni, M. Dionigi, C. Tomassoni, and R. Sorrentino, "Design of a compact 3D printed coaxial filter," in *Proc. 48th Eur. Microw. Conf. (EuMC)*, Sep. 2018, pp. 280–283.

[27] A. L. Borja, A. Belenguer, H. Esteban, and V. E. Boria, "Design and performance of a high-Q narrow bandwidth bandpass filter in empty substrate integrated coaxial line at Ku-band," *IEEE Microw. Wireless Compon. Lett.*, vol. 27, no. 11, pp. 977–979, Nov. 2017.

[28] L. Martinez, J. A. Martinez, A. L. Borja, H. Esteban, V. E. Boria, and A. Belenguer, "Compact bandpass filter in empty substrate integrated coaxial line," in *Proc. 48th Eur. Microw. Conf. (EuMC)*, Sep. 2018, pp. 162–165.

[29] L. Martinez, A. Belenguer, V. E. Boria, and A. L. Borja, "Compact folded bandpass filter in empty substrate integrated coaxial line at *S*-band," *IEEE Microw. Wireless Compon. Lett.*, vol. 29, no. 5, pp. 315–317, May 2019.

[30] J. M. Merello, V. Nova, C. Bachiller, J. R. Sanchez, A. Belenguer, and V. E. Boria, "Miniaturization of power divider and 90° hybrid directional coupler for C-Band applications using empty substrate-integrated coaxial lines," *IEEE Trans. Microw. Theory Techn.*, vol. 66, no. 6, pp. 3055–3062, Jun. 2018.

[31] A. R. Barnes, A. Boetti, L. Marchand, and J. Hopkins, "An overview of microwave component requirements for future space applications," in *Proc. Eur. Gallium Arsenide Other Semiconductor Appl. Symp.*, Oct. 2005, pp. 5–12.

[32] M. N. Sweeting, "Modern small satellites-changing the economics of space," *Proc. IEEE*, vol. 106, no. 3, pp. 343–361, Mar. 2018.

[33] A. E. Mostrah, B. Potelon, E. Rius, C. Quendo, J. Favennec, H. Leblond, H. Yahi, and J. Cazaux, "C-band inductive post SIW alumina filter for a space application. Experimental analysis of the thermal behavior," in *Proc. Asia–Pacific Microw. Conf.*, Dec. 2010, pp. 103–106.

[34] X.-P. Chen and K. Wu, "Substrate integrated waveguide filters: Practical aspects and design considerations," *IEEE Microw. Mag.*, vol. 15, no. 7, pp. 75–83, Nov. 2014.

[35] T. Djerafi, K. Wu, and D. Deslandes, "A temperature-compensation technique for substrate integrated waveguide cavities and filters," *IEEE Trans. Microw. Theory Techn.*, vol. 60, no. 8, pp. 2448–2455, Aug. 2012.

[36] T. Martin, A. Ghiotto, T.-P. Vuong, and F. Lotz, "Self-Temperature-Compensated air-filled substrate-integrated waveguide cavities and filters," *IEEE Trans. Microw. Theory Techn.*, vol. 66, no. 8, pp. 3611–3621, Aug. 2018.

[37] *ESA Requirements and Standards Division ESTEC*, Space Engineering Testing, document ECSS-E-ST-10-03C., 2012.

[38] O. Monerris, E. Diaz, J. Ruiz, and V. E. Boria, "Automatic, calibrated and accurate measurement of S-parameters in climatic chamber," *IEEE Microw. Wireless Compon. Lett.*, vol. 25, no. 6, pp. 412–414, Jun. 2015.

VICENTE NOVA received the M.Sc. degree in communication engineering from the Universitat Politécnica de Valéncia, in 2016, and the master's degree Project on ESICL broadband transitions. His current research interests include optimization and design of substrate integrated microwave devices, design and manufacture of SICs lines, design of reconfigurable devices using anisotropic materials, and additive manufacturing processes.

CARMEN BACHILLER MARTIN (Member, IEEE) received the M.Sc. degree in telecommunication engineering and the Ph.D. degree in telecommunication from the Universitat Politécnica de Valéncia, in 1996 and 2010, respectively. She has worked as a Project Engineer with ETRA I+D Company, from 1997 to 2001, in research and development on automatic traffic control, public transport management, and public information systems using telecommunication technology. In 2001, she joined the Communication Department, Universitat Politécnica de Valéncia, as an Assistant Lecturer, where she has been an Associate Professor, since 2011. She is teaching electromagnetism theory. She has participated in several teaching innovation projects and technological heritage studies. Her current research interests include modal methods for electromagnetic analysis, optimization and design of passive microwave structures, analysis and design of substrate integrated transmission lines and circuits, and power effects in passive waveguide systems.

JUAN ANGEL MARTÍNEZ (Member, IEEE) received the degree in telecommunications engineering from the Universidad de Castilla-La Mancha (UCLM), Cuenca, Spain, in 2012, and the master's degree in research telecommunications (major in electronics and communications) from University Miguel Hernandez (UMH), Elche, Spain, in 2013. In 2013, he joined the Universidad de Castilla-La Mancha, where he was a Research Assistant with the Group de Electromagnetismo Aplicado. His current research interests include computational electromagnetics and the analysis and the synthesis of passive microwave circuits and antennas, and substrate integrated waveguide (SIW) devices analysis and their applications.

HÉCTOR ESTEBAN GONZÁLEZ (Senior Member, IEEE) received the degree in telecommunications engineering from the Polytechnic University of Valencia (UPV), Spain, in 1996, and the Ph.D. degree, in 2002. He collaborated with the Joint Research Center, European Commission, Ispra, Italy. In 1997, he was with the European Topic Center on Soil (European Environment Agency). He rejoined UPV, in 1998. His research interests include methods for the full-wave analysis of open-space and guided multiple scattering problems, CAD design of microwave devices, electromagnetic characterization of dielectric and magnetic bodies, the acceleration of electromagnetic analysis methods using the wavelets and the FMM, and the design and implementation of communication devices in substrate integrated technologies.

JOSÉ MANUEL MERELLO received the B.Sc. degree in communication engineering from the Universitat Politécnica de Valéncia, in 2017. He is currently pursuing the M.Sc. degree in communication engineering. He made his final degree project on analysis and design of passive devices on ESICL.

ÁNGEL BELENGUER MARTÍNEZ (Senior Member, IEEE) received the degree in telecommunications engineering and the Ph.D. degree from the Universitat Politécnica de València (UPV), Valencia, Spain, in 2000 and 2009, respectively. In 2000, he joined the Universidad de Castilla-La Mancha, Cuenca, Spain, where he is currently a Professor Titular de Universidad with the Departamento de Ingenieria Electrica, Electronica, Automatica y Comunicaciones. He has authored or coauthored more than 50 papers in peer-reviewed international journals and conference proceedings. His current research interests include methods in the frequency domain for the full-wave analysis of open-space and guided multiple scattering problems, EM metamaterials, and empty substrate integrated waveguide (ESIW) devices and their applications. He serves as a Reviewer for several international technical publications.

OSCAR MONERRIS received the master's degree from the Universidad Politécnica de Valencia, Valencia, Spain, in 2009. His current research interests include high-RF power effects in space applications, including the analysis of multicarrier and modulated signals.

VICENTE E. BORIA (Fellow, IEEE) was born in Valencia, Spain, in May 1970. He received the Ingeniero de Telecomunicación (Hons.) and Doctor Ingeniero de Telecomunicación degrees from the Universidad Politécnica de Valencia, Valencia, Spain, in 1993 and 1997, respectively. In 1993, he joined the Departamento de Comunicaciones, Universidad Politécnica de Valencia, where he has been a Full Professor, since 2003. From 1995 to 1996, he was holding a Spanish Trainee position with the European Space Research and Technology Centre, European Space Agency (ESTEC-ESA), Noordwijk, The Netherlands, where he was involved in the area of EM analysis and design of passive waveguide devices. He has authored or coauthored ten chapters in technical textbooks, 180 articles in refereed international technical journals, and over 200 papers in international conference proceedings. His current research interests include analysis and automated design of passive components, left-handed and periodic structures, and the simulation and measurement of high-power effects in passive waveguide systems. He has been a member of the IEEE Microwave Theory and Techniques Society (IEEE MTT-S) and the IEEE Antennas and Propagation Society (IEEE AP-S), since 1992. He is also a member of the Technical Committees of the IEEE-MTT International Microwave Symposium and of the European Microwave Conference. He acts as a regular Reviewer of the most relevant IEEE and IET technical journals on his areas of interest. He was an Associate Editor of the IEEE Microwave and Wireless Components Letters, from 2013 to 2018, and *IET Electronics Letters*, from 2015 to 2018. He currently serves as a Subject Editor (Microwaves) for *IET Electronics Letters*, and an Editorial Board Member for the *International Journal of RF and Microwave Computer-Aided Engineering*.